



e-ISSN: 2548-060X

International Journal of Energy Applications and Technologies

journal homepage: www.dergipark.gov.tr/ijeat

Original Research Article

Thermal efficiency evaluation of an organic Rankine cycle with n-pentane as working fluid

Sadık Ata^{1*}, Ali Kahraman², Remzi Şahin¹¹ Mechanical Engineering Department, KTO Karatay University, Faculty of Engineering, TURKEY² Energy Systems Engineering Department, Necmettin Erbakan University, Faculty Of Engineering and Architecture, TURKEY

ARTICLE INFO

* Corresponding author
sadik.ata@karatay.edu.trReceived July 17, 2018
Accepted May 20, 2019Published by Editorial Board
Members of IJEAT© This article is distributed by
Turk Journal Park System under
the CC 4.0 terms and conditions.

doi: 10.31593/ijeat.444464

ABSTRACT

In this study, the effect of evaporation pressure and superheating temperature on system performance was determined in the Organic Rankine Cycle (ORC) model designed using n-pentane fluid. EES (Engineering Equation Solver) software design using 9 different conditions have been identified. In the first model where the evaporation pressure was between 250 kPa and 400 kPa, the efficiency of ORC was determined under five different constant superheating temperatures. In the second model, the evaporation pressure was determined as 4 different constant values and the temperature of the superheating temperature was changed between 0 °C and 20 °C. N-pentane, which is widely used in ORC geothermal applications, has been determined as working fluid. Within the scope of geothermal applications, the heat source temperature is assumed to be constant at 120 °C. Condenser pinch point temperature difference is taken as 3 °C. As a result of the study, the data obtained from two different models were evaluated separately. When the superheating temperature is not applied, turbine work increases by 35% as the evaporation pressure rises from 250 kPa to 400 kPa. In addition, thermal efficiency also increased by 26%. When the evaporation pressure is constant at 250 kPa, the turbine work increased by 7.32% due to the increase of the superheating temperature from 0 °C to 20 °C. However, with the increase of heat input, thermal efficiency decreased by 1.38%. In the ORC system using N-pentane, it is stated that application of the superheating temperature reduces the performance. In the study, the highest thermal efficiency (12.59%) was achieved at the evaporation pressure of 400 kPa in the case of not applying superheating. The main purpose of this study was to evaluate the thermal efficiency of n-pentane fluid used in the geothermal applications of ORC under different evaporation pressure and overheating temperatures.

Keywords: organic Rankine cycle (ORC); thermal efficiency; superheating; n-Pentane

1. Introduction

Organic Rankine Cycles work on the same principle as Rankine cycles in terms of thermodynamics. Rankine cycles are conventional steam turbines where electricity is generated from the heat and require high temperature and pressure resources depending on operating conditions. Unlike the Rankine cycle, the organic Rankine cycle is a power system in which organic fluids are used instead of water which is fluid in low temperature ranges. Because of

the evaporation of the organic fluid at lower temperatures, electric fields are possible from lower temperature heat sources. Thanks to these properties, energy production can be used more efficiently in non-economic industrial waste heat, geothermal heat, solar energy, oil and gas fields [1].

Kaska [2] have analyzed energy and exergy analysis of waste heat-driven Organic Rankine Cycle. The effect of the evaporator/condenser pressure, superheating and sub-cooling on energy and exergy efficiency is shown. The order of the

components with the most exergy destruction is evaporator, turbine, condenser and pump. It has been found that the effect of the evaporative pressure on both energy and exergy efficiency is great. Lecompte et al. [3], studied the second law-based thermodynamic performance analysis for non-superheated subcritical Organic Rankine cycle using the zeotropic mixture as the organic fluid. REFPROP9.0 provides thermo-physical data of zeotropic mixture and pure fluids. R245fa-pentane, R245fa-R365mfc, isopentane-isohexane, isopentane-cyclohexane, isobutane-isopentane and pentane-hexane selected as zeotropic mixture. The second law is used as the optimization criterion. Compared with pure fluids, the efficiency of the second law was increased by 7.1% and 14.2%. Le et al. [4], optimized the performance of a supercritical ORC system with low temperature power generation using fluids with low global warming potential (GWP) as the organic fluid. Commonly used R134a fluid is used for comparison. Hot water at 150 °C and 5 bar pressure was used as the heat source medium. The thermodynamic performance comparison of the supercritical Organic Rankine Cycle was performed using the Ranking method and the exergy method using different organic fluids. For the highest available efficiency of the system; R152a was obtained for 11.6% for simple cycle and 13.1% for regenerative cycle. The best organic fluids for system efficiency optimization are R32 for simple cycle and R152a for regenerative cycle. Javanshir and Sarunac [5], assessed the thermodynamic performance of the simple subcritical and super-critical Organic Rankine Cycle. They have analyzed organic fluids over various operating conditions and have made the best fluid choice. Epsilon Professional software was used for thermodynamic modeling. The efficiency of isentropic fluids is higher than that of dry and wet fluids.

The design of the small scale Organic Rankine cycle system and the control conditions for low grade heat recovery applications were conducted through experimental investigations by Li et al. [6]. For the ORC system, the R245fa was selected as the organic fluid. The effects of the condenser cooling water temperature and the performance of the hot R245fa at the turbine inlet and on the cycle have been measured and analyzed. ORC expansion is guaranteed with some security operations. The thermal expansion of the heated R245fa was controlled to remain constant. In the constant heat source parameters (temperature and flow rate), turbo expander net output power and cycle efficiency are reduced with coolant water temperature. Under the specified specific test conditions, when the cooling water temperature was set at 23.0 °C and the pressure ratio was set at 7.3, the maximum turboexpanding power generation was able to achieve 5.405 kW.

Hydrofluorinated ethers containing HFE7000, HFE7100 and HFE7500 were analyzed using the Organic Rankine Cycle as the organic fluid under fixed external conditions by Wang et al. [7]. They developed a computer program to compare the first and second efficiency laws, net power output, turbine inlet temperature increase and turbine size factor. Thermodynamic analyzes of the organic fluids tested under the turbine inlet temperature were performed using the Engineering Equation Solver (EES) computer program. It was found that HFE7000 produces maximum thermodynamic efficiency and gives the best result in terms of net power under given conditions. The HFE7000 organic fluid has been found to have the lowest turbine size compared to HFE7100 and HFE7500. In the ORC, HFE7000 has been proposed to be used as a organic fluid for low temperature heat conversion. Li et al. [8] have used the R1234ze(E) fluid for a 100-200 °C heat source to optimize critical and transcritical Organic Rankine cycles and thermodynamic performance analyzes. The thermo-physical properties of R1234ze(E) fluid were calculated using REFPROP. It has been found that the trans critical ORC system has higher system efficiency than the subcritical ORC system, but has lower heat absorption capacity. The maximum power output of R1234ze (E) is 31.4% higher than R245fa and 25.8% higher than R600 for 100-167 °C heat source.

Feng et al. [9] investigated the test and study characteristics of the Organic Rankine cycle using a scroll compressor. R123 was selected as the working fluid. Based on the measured temperatures and pressures, entropy and entropy corresponding to each state were obtained with NIST REFPROP. With the help of experimental data, the pump power consumption, isentropic efficiency and recycle rate were obtained as 0.21-0.32 kW, 26.76-53.96% and 14-32% respectively. When the heat transfer coefficient of the evaporator and the condenser is 200-400 and 450-2000 W/m²K respectively, it is found that the expansion isentropic and generator efficiency are in the range of 69.10-85.17% and 60-73% respectively.

In this study, the role of evaporation pressure and superheating temperature in ORC performance was determined by the thermodynamic design model. In the thermodynamic design model prepared with EES, n-pentane was selected as the organic fluid. In geothermal power plants with ORC technology, the effect of the n-pentane fluid, which is widely used as organic fluid, on the system has been determined. Within the scope of the study two different models were created. In the first model, the superheating temperature is kept constant to detect the effect of the evaporation pressure on the system. In the second model, the results of the change in superheating temperature under constant evaporation pressure were examined.

In both models, the amount of heat requirement, work done by the turbine, turbine inlet-outlet temperature and thermal efficiency values were determined. In the study, considering the thermo-physical properties of the n-pentane fluid, the input parameters were determined so as not to be in contradiction with the laws of thermodynamics. The main purpose of this work is to determine the effect of the n-pentane fluid on the system performance, which is used extensively in the ORC application field, together with the evaporation pressure and superheating temperature changes.

2. Material and Method

The working principle of the Organic Rankine Cycle and the T-s diagram are given in Fig.1.

1-2: Isentropic compression in the pump, 2-3: Heat input at constant pressure in evaporator, 3-4: Isentropic expansion in turbine, 4-1: Heat output at constant pressure in condenser.

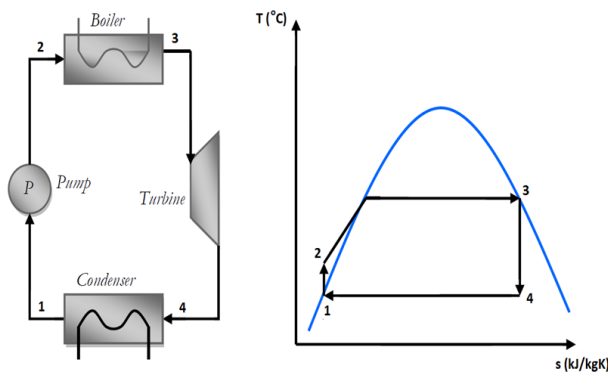


Fig. 1. ORC Working principle and T-s diagram [10]

The physical and environmental properties of the n-pentane fluid determined in the study are given in Table 1. It is noteworthy that it has a low boiling temperature and that ODP value which is important from environmental care is 0.

Table 1. Physical and environmental properties n-pentane used in design [11]

Properties	n-pentane
ds/dT	Dry fluid
Molecular Mass (g/mol)	72.15
Normal Boiling Point (°C)	36.1
Critical Temperature (°C)	196.6
Critical Pressure (MPa)	3.37
ASHRAE 34 safety group	A3
ODP	0
GWP	20

When the slope of the saturation curves in the T-s diagrams of the fluids is positive, it is called the dry fluid. The T-s diagram of the n-pentane fluid which is a dry fluid is given in Fig.2.

Within the scope of the study two different models were created. For each of the prepared models, 9 different thermodynamic states were analyzed. For all situations; pump inlet temperature 20 °C, cooling water temperature 17

°C, hot source temperature 120 °C. In addition, the isentropic efficiency of the turbine and pump is taken as 85%.

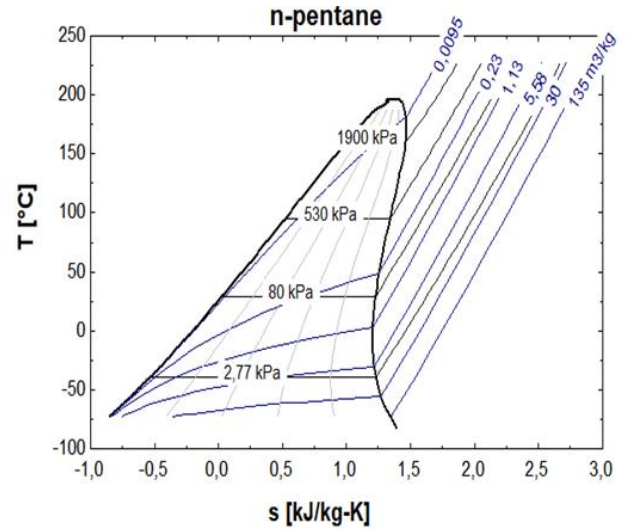


Fig. 2. T-s diagram of n-pentane fluid

Thermodynamic design models were created using EES. The equations for energy analysis are given in Equation 1-9. These equations were processed in EES program and energy analysis was started. In the program, the values which are accepted as fixed first are indicated. Figure 3 presents a flow diagram describing the working principle of two different models. Energy analysis was performed based on this flow diagram.

Energy Analysis:

$$(Q_{in} - Q_{out}) + (W_{in} - W_{out}) = h_e - h_i \quad (1)$$

Pump ($q = 0$)

$$W_{pump, in} = h_2 - h_1 \quad (2)$$

$$W_{pump, in} = v(P_2 - P_1) \quad (3)$$

where

$$h_1 = h_f @ P_1 \text{ and } v \cong v_1 = v_f @ P_1 \quad (4)$$

Boiler ($w = 0$):

$$Q_{in} = h_3 - h_2 \quad (5)$$

Turbine ($q = 0$):

$$W_{turbine} = h_3 - h_4 \quad (6)$$

Condenser ($w = 0$):

$$Q_{out} = h_4 - h_1 \quad (7)$$

The energy efficiency of the Rankine cycle

$$\eta_{th} = \frac{W_{net}}{Q_{in}} = 1 - \frac{Q_{out}}{Q_{in}} \quad (8)$$

where

$$W_{net} = Q_{in} - Q_{out} = W_{turb, out} - W_{pump, in} \quad (9)$$

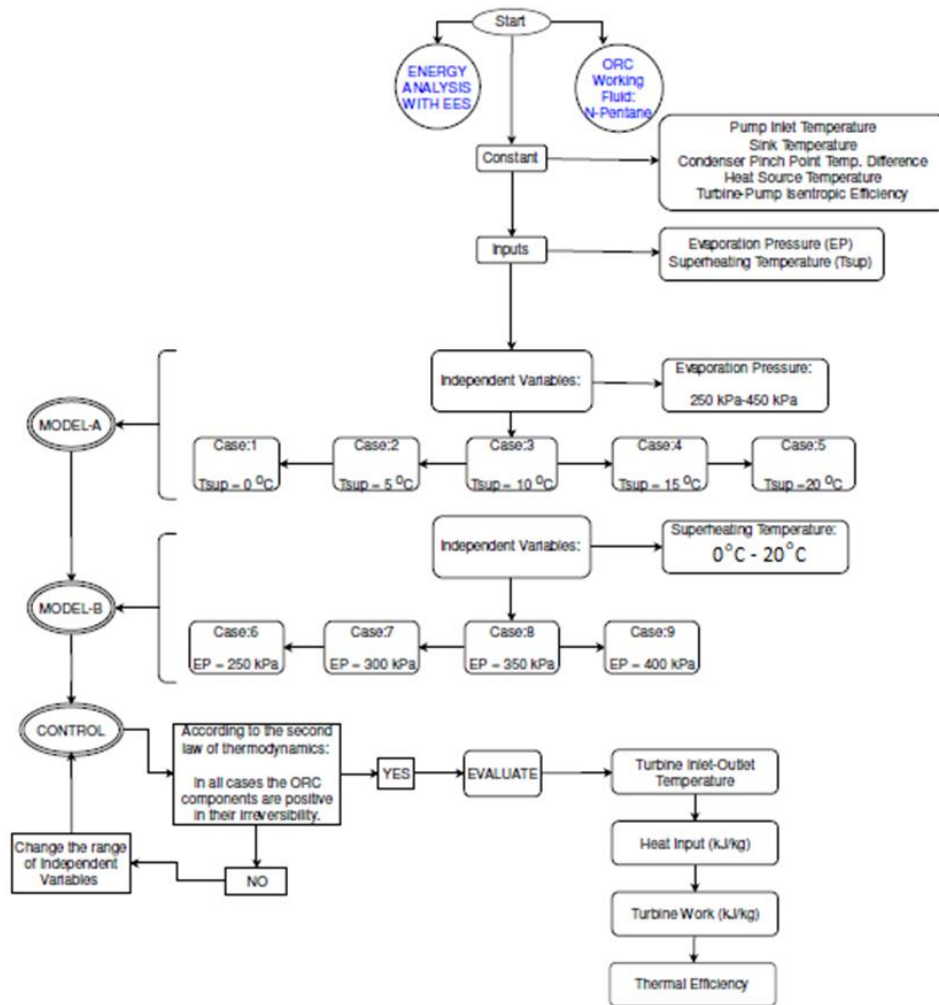


Fig. 3. Flow chart for Simulation of ORC System with N-Pentane

The purpose of this study is to demonstrate the effect of evaporation pressure and superheating temperature on ORC performance. In determining the amount of heat required in the system, the importance of the evaporation pressure is specified. In evaporative pressure change, a system that does not have a superheating temperature and a system that has a fixed superheating temperature of 5, 10, 15, and 20 °C have been examined. Secondly, the influence of the superheating temperature change on the system under fixed evaporation pressures of 250-300-350 and 400 kPa was determined. The performance of the n-pentane fluid, which is used in ORC application field, at different evaporation pressures and superheating temperatures, has been tried to be explained by energy analysis.

3. Model Validation

The data obtained in order to determine the accuracy of the simulation study with EES were compared with another study (Ref. [10]) in the same working conditions. N-pentane fluid was used in the study. Hot source temperature 90 °C,

sink temperature 28 °C, evaporator temperature 75 °C, condenser temperature 35 °C, pump efficiency 80%, the total efficiency (mechanical+isentropic) of the turbine 44% is taken. The results of two studies in the same study parameters are given in Table 2. The results are very close to each other.

Table 2. Comparison between the present results and those from Ref. [10].

Performance parameters	Ref. [10]	Present Work
Working Fluid	n-Pentane	n-Pentane
Heat Input [kJ/kg]	421.41	421.8
Turbine Work [kJ/kg]	18.86	18.84
Thermal efficiency [%]	4.367	4.359

4. Results and Discussion

In this study, the input parameters were determined for the selected n-pentane fluid by checking the compatibility with the second law of thermodynamics. A much lower evaporation pressure range was determined compared to the evaporation pressures of the classic Rankine cycle.

I) MODEL-A

In the first model, the system performance was examined by changing the evaporation pressure between 250 kPa and 400 kPa. The thermodynamic design model has been prepared

separately for the following 5 different situations. For all cases, the amount of heat required for the system, turbine work, turbine inlet-outlet temperatures and thermal efficiency values are determined separately. With 75 input numerical test values, 375 numerical output values for each case were obtained. The analysis of model A was done with a numerical output value of 1875 for 5 different situations in total. These situations are;

- No superheating
- 5 °C degree of superheat
- 10 °C degree of superheat
- 15 °C degree of superheat
- 20 °C degree of superheat

Figure 4 shows the effect of evaporation pressure change on the amount of heat requirement for different superheating temperatures. In all cases, as the evaporation pressure increases, the system seems to require more heat. As the evaporation pressure increased from 250 kPa to 400 kPa, the heat requirement increased by 28 kJ/kg for a no superheating system, while it increased by 31 kJ/kg for a system with constant 20 °C degree of superheat.

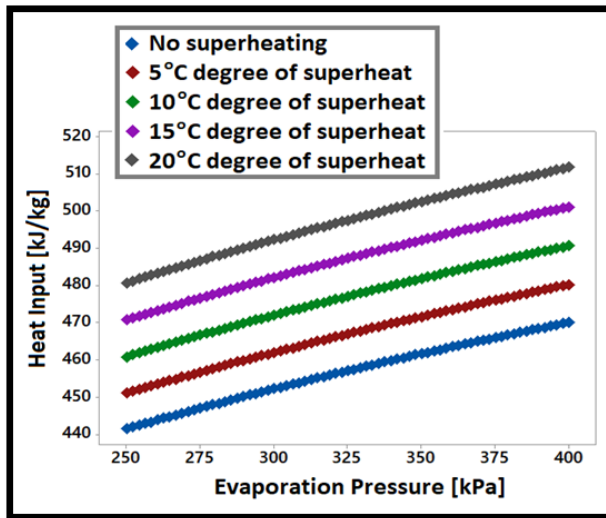


Fig. 4. Change of heat input with evaporation pressure

Figure 5 shows the effect of evaporation pressure change on turbine inlet temperature for different superheating temperatures conditions. In all cases, as the evaporation pressure increases, the turbine inlet temperature increases. When the system without superheating is examined, the turbine inlet temperature for the 250 kPa evaporation pressure is 65.51 °C, while for 400 kPa this value has risen to 83.54 °C. The highest turbine inlet temperature value (103.4 °C), constant 20 °C superheating temperature and 400 kPa evaporation pressure.

Figure 6 shows the effect of evaporative pressure change on turbine work for different superheating temperature conditions. In all cases, as the evaporation pressure increases,

the turbine work seems to increase. When the system without superheating was examined, the turbine work for the 250 kPa evaporation pressure was 44.21 kJ/kg, while for 400 kPa this value increased to 59.81 kJ/kg. For different superheating temperatures, the turbine work seems to give a closer result than the heat requirement.

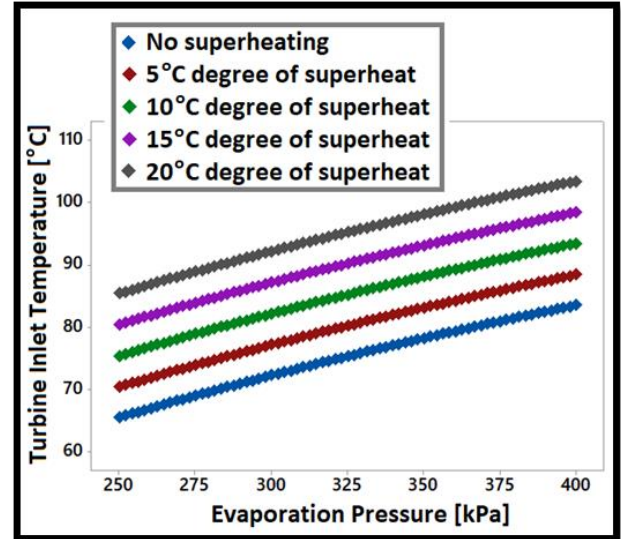


Fig. 5. Change of turbine inlet temperature with evaporation

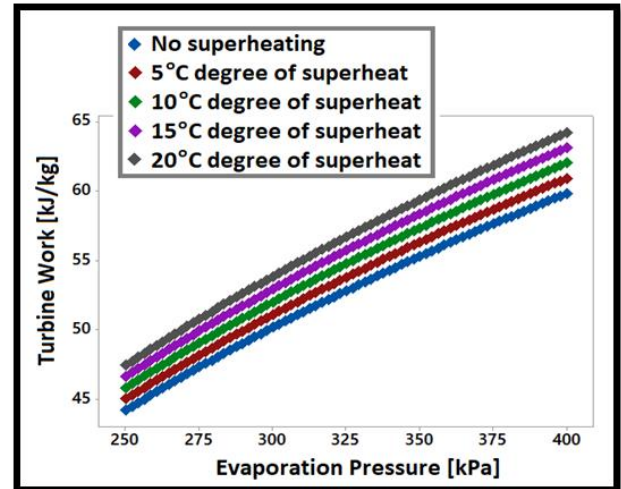


Fig. 6. Change of turbine work with evaporation pressure

Figure 7 shows the effect of evaporation pressure change on the turbine outlet temperature. As the evaporation pressure increases, the turbine outlet temperature increases. When the system without superheating is examined, the turbine outlet temperature for the 250 kPa evaporation pressure is 36.07 °C, while for 400 kPa, this value has increased to 43.66 °C. For a 400 kPa evaporation pressure, the turbine inlet temperature was reported to be 103.4 °C when the system had a constant 20 °C superheating temperature on Fig.4. Under the same values, the turbine outlet temperature was calculated as 64.19 °C.

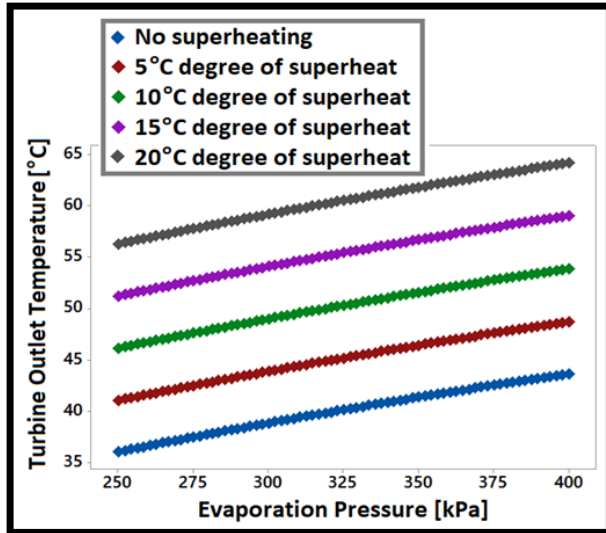


Fig. 7. Change of turbine outlet temperature with evaporation pressure

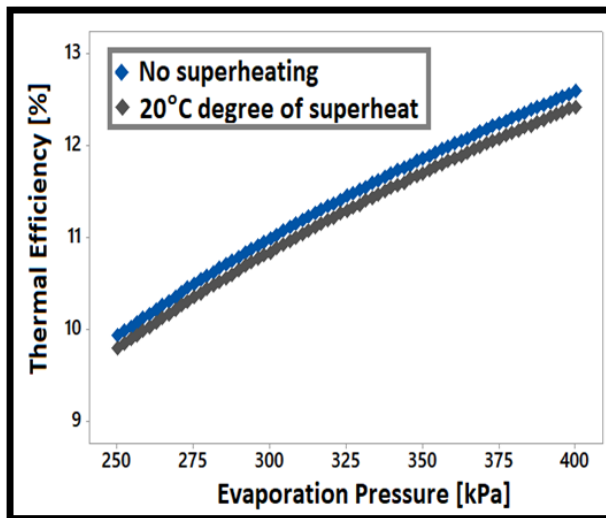


Fig. 8. Change of thermal efficiency with evaporation pressure

Figure 8 shows the effect of the evaporation pressure change on the thermal efficiency. As the evaporation pressure increases, the thermal efficiency increases. Since the different superheating temperatures give very close results, two situations have been mentioned that are more obvious. When the system without superheating was examined, the thermal efficiency for the 250 kPa evaporation pressure was 9.93%, while it increased to 12.59% for 400 kPa. When the system has a constant 20 °C superheating temperature, the thermal efficiency appears to drop slightly for all pressures. Figure 8 shows the effect of the evaporation pressure change on the thermal efficiency. As the evaporation pressure increases, the thermal efficiency increases. Since the different superheating temperatures give very close results, two situations have been mentioned that are more obvious. When the system without superheating was examined, the thermal efficiency for the 250 kPa evaporation pressure was 9.93%, while it increased to 12.59% for 400 kPa. When the

system has a constant 20 °C superheating temperature, the thermal efficiency appears to drop slightly for all pressures.

II) MODEL-B

In the second model, the system performance was examined by changing the superheating temperature between 0 °C and 20 °C. The thermodynamic design model is prepared separately for the following 4 different situations. For all cases, the amount of heat required for the system, turbine work, turbine inlet-outlet temperatures and thermal efficiency values are determined separately. With 100 input numerical test values, 500 numerical output values for each case were obtained. The analysis of model B was made with 2000 numerical output values for 4 different situations in total. These situations are;

- 250 kPa evaporation pressure
- 300 kPa evaporation pressure
- 350 kPa evaporation pressure
- 400 kPa evaporation pressure

Figure 9 shows the effect of superheating temperature change on the amount of heat requirement for different evaporation pressure (P_e) conditions. In all cases, as the superheating temperature increases, the system seems to require more heat. For a 250 kPa constant evaporation pressure, the heat requirement for the system is 441.4 kJ/kg when there is no superheating, while this value rises to 480.7 kJ/kg when the superheating temperature is 20 °C.

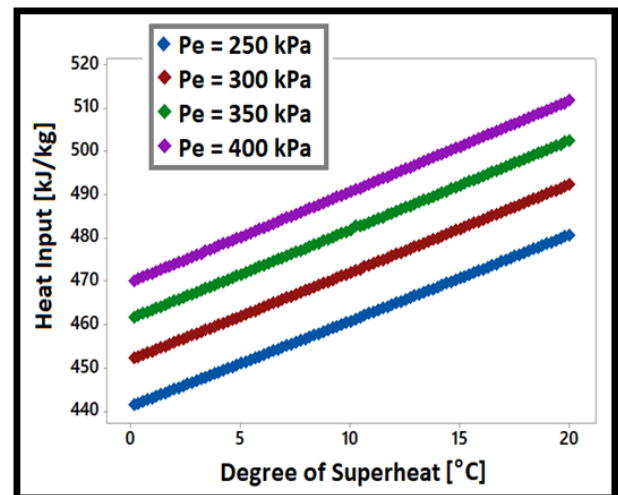


Fig. 9. Change of heat input with superheating temperature

Figure 10 shows the effect of superheating temperature change on turbine inlet temperature for different evaporative pressure situations. For 250 kPa constant evaporation pressure, the turbine inlet temperature is 65.41 °C when there is no superheating, while this value increases to 85.41 °C with 20 °C superheating temperature.

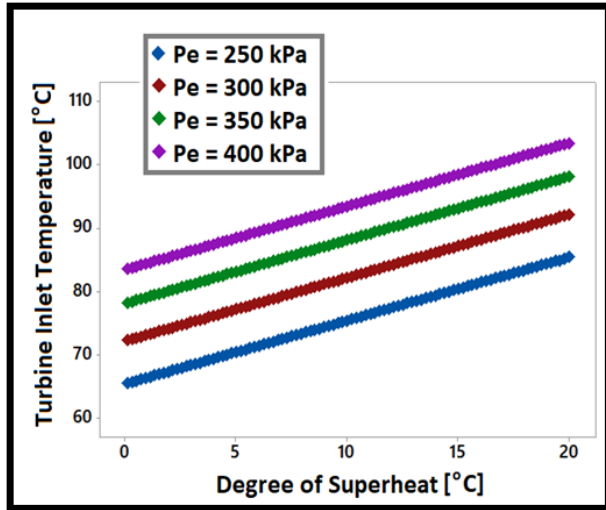


Fig. 10. Change of turbine inlet temperature with superheating temperature

Figure 11 shows the effect of the superheating temperature change on turbine work for different evaporation pressure states. In all cases, the turbine work seems to increase as the superheating temperature increases. For 250 kPa constant evaporation pressure, turbine work value is 44.21 kJ/kg when there is no superheating, while this value increases to 47.45 kJ/kg when it is 20 °C superheating.

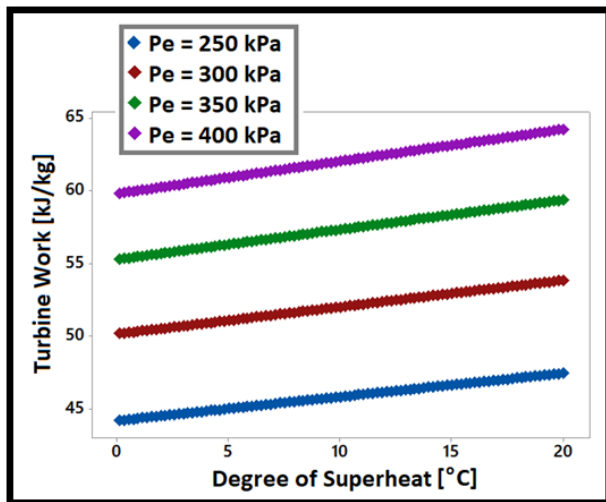


Fig. 11. Change of turbine work with superheating temperature

Figure 12 shows the effect of the superheating temperature change on the turbine outlet temperature for different evaporation pressure states. In all cases, the temperature of the turbine outlet increases as the superheating temperature increases. For a 250 kPa constant evaporation pressure, when there is no superheating, the turbine outlet temperature is 36.07 °C, while at 20 °C superheating, this value rises to 56.29 °C.

Figure 13 shows the effect of the superheating temperature change on the thermal efficiency for different evaporation pressure states. For all cases, it is seen that as the

superheating temperature increases, the thermal efficiency decreases slightly. For 250 kPa constant evaporation pressure, the thermal efficiency is 9.93% when there is no superheating, while it decreases to 9.79% when the superheating temperature is 20 °C.

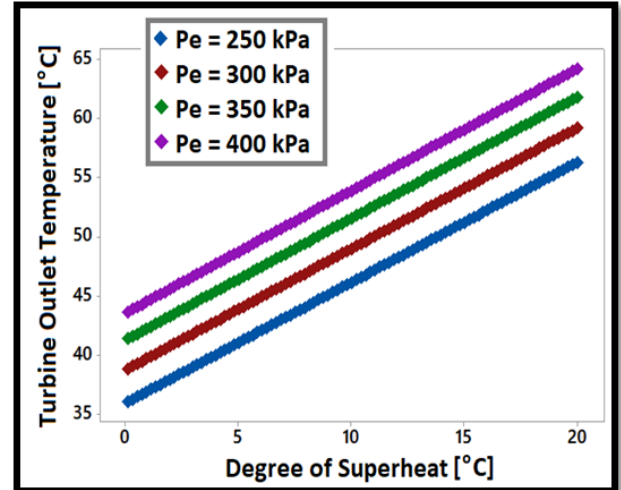


Fig. 12. Change of turbine outlet temperature with superheating temperature

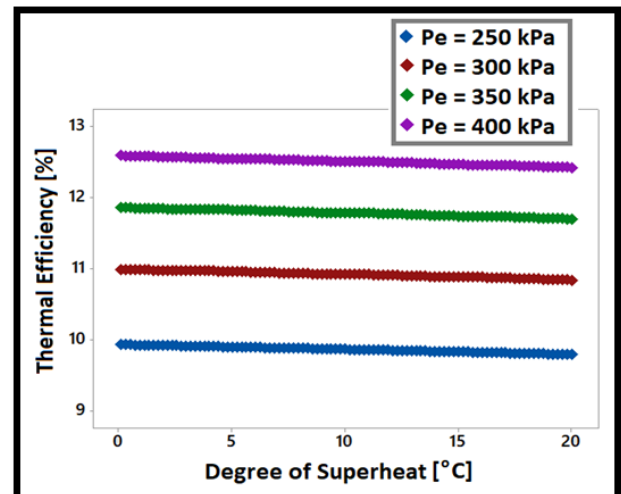


Fig. 13. Change of thermal efficiency with superheating temperature

5. Conclusion

In this study, the energy analysis of the n-pentane fluid, which is used too much as the organic fluid in ORC application, is done. On the n-pentane fluid, the effect of evaporation pressure and superheating temperature was evaluated with two different models prepared. The thermodynamic design model is based on the integrated use of EES.

Five different situations were analyzed in the prepared first model. The effect of the evaporation pressure on the system at different superheating temperatures is determined. If the first case without superheating is taken into consideration, increasing the 250 kPa evaporation pressure to 400 kPa

increases the thermal efficiency of the system from 9.93% to 12.59%. However, the amount of heat requirement for the system increases from 441.4 kJ/kg to 470.1 kJ/kg. When the system with 5 °C superheating temperature is considered, the thermal efficiency has increased from 9.90% to 12.55% as the evaporation pressure is increased from 250 kPa to 400 kPa. The amount of heat required for the system increases from 451 kJ/kg to 480.2 kJ/kg. Evaporation pressure was found to increase the thermal efficiency of the system at all constant superheating temperatures, but at the same time it increased the amount of heat requirement in the system.

In the second model, the evaporation pressures are assumed to be constant and the effect of superheating temperatures is discussed in more detail. Four different situations have been analyzed. For the 250 kPa constant evaporation pressure, the thermal efficiency of the system without superheating is 9.93%, while the thermal efficiency at the 20 °C superheating temperature is 9.79%. For the 400 kPa constant evaporation pressure, the thermal efficiency of the system with no superheating is 12.59%, while the thermal efficiency at 20 °C superheating temperature is 12.42%. It has been seen that the increase of the superheating temperature slightly reduces the thermal efficiency value at all constant pressure values.

As a result, it is presented that the energy analysis of the ORC system containing n-pentane fluid can be successfully applied with the thermodynamic design model developed with EES in this study.

Acknowledgments

This study constitutes part of the ongoing PhD thesis of Sadık Ata.

References

- [1] Ağırkaya, O., 2015, "Jeotermal Enerji Kaynaklı Organik Rankine Çevriminin Modellenmesi ve Analizi", Master Thesis, İstanbul Teknik University, Graduate School of Natural Sciences, İstanbul, Turkey.
- [2] Kaska, O., 2014, "Energy and exergy analysis of an organic Rankine for power generation from waste heat recovery in steel industry", *Energy Conversion and Management*, 77, 108-117.
- [3] Lecompte, S., Ameel, B., Ziviani, D., Broek, M., Paepe, M., 2014, "Exergy analysis of zeotropic mixtures as working fluids in Organic Rankine Cycles", *Energy Conversion and Management*, 85, 727-739.
- [4] Le, V., Feidt, M., Kheiri, A., Pelloux-Prayer, S., 2014, "Performance optimization of low-temperature power generation by supercritical ORCs (organic Rankine cycles) using low GWP (global warming potential) working fluids", *Energy*, 67, 513-526.
- [5] Javanshir, A., Sarunac, N., 2017, "Thermodynamic analysis of a simple Organic Rankine Cycle", *Energy*, 118, 85-96.
- [6] Li, L., Ge, Y., Tassoua, S., 2017, "Experimental Study on a small-scale R245fa Organic Rankine cycle system for low-grade thermal Energy Recovery", *Energy Procedia*, 105, 1827-1832.
- [7] Wang, H., Li, H., Wang, L., Bu, X., 2017, "Thermodynamic Analysis of Organic Rankine Cycle with Hydrofluoroethers as Working Fluids", *Energy Procedia*, 105, 1889-1894.
- [8] Li, J., Liu, Q., Ge, Z., Duan, Y., Yang, Z., 2017, "Thermodynamic performance analyses and optimization of subcritical and transcritical organic Rankine cycles using R1234ze(E) for 100–200°C heat sources", *Energy Conversion and Management*, 149, 140-154.
- [9] Feng, Y.Q., et al., 2017, "Operation characteristic of a R123-based organic Rankine cycle depending on working fluid mass flow rates and heat source temperatures", *Energy Conversion and Management*, 131, 55-68.
- [10] Tchanche B.F., 2010, "Low-Grade Heat Conversion into Power Using Small Scale Organic Rankine Cycles", Doctoral Thesis, Department of Natural Resources and Agricultural Engineering, Agricultural University of Athens, AUA.
- [11] Calm J.M., Hourahan, G.C., 2007, "Refrigerant Data Update", *Heating/Piping/Air Conditioning Engineering*, 79(1), 50-64.